Time variations of the core surface magnetic field from Swarm and ground observatories: Latest results and alternative inversion schemes

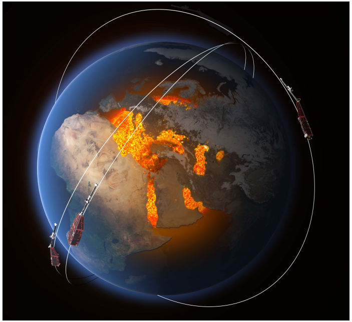

C. Finlay, N. Olsen, M. Hammer, C. Kloss,

O. Barrois and L. Tøffner-Clausen

DTU Space, Technical University of Denmark

P. Livermore

Dept. Earth and Environment, University of Leeds

DTU Space
National Space Institute

European Research Council
Established by the European Commission

Motivation: Magnetic field variations probe core dynamics

- Core motions drive observed changes in Earth's magnetic field:

$$\underbrace{\frac{\partial \mathbf{B}}{\partial t}}_{\text{Secular variation (SV)}} = \underbrace{\nabla \times (\mathbf{u} \times \mathbf{B})}_{\substack{\text{Advection \& stretching}\\ \text{by core flow}}} + \underbrace{\eta \nabla^2 \mathbf{B}}_{\text{Ohmic diffusion}}$$

- Detailed knowledge of SV, and its time variations, thus provides us with valuable constraints on core dynamics

- **This talk:**
  SV as observed by satellites; past 5 yrs by the *Swarm* mission

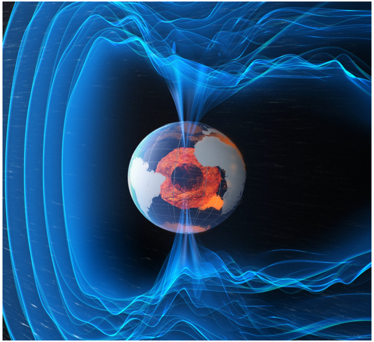

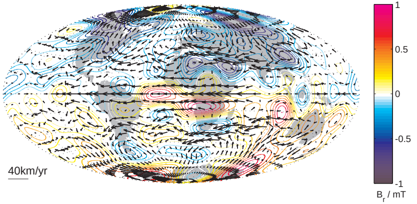

Swarm satellite trio: Five years measuring Earth's magnetic field

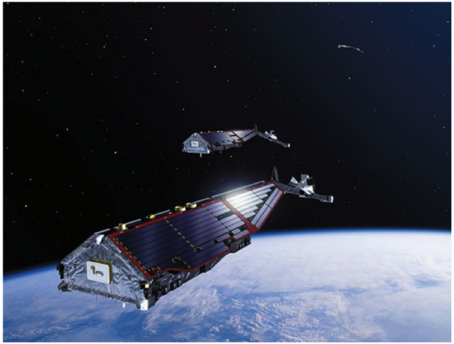

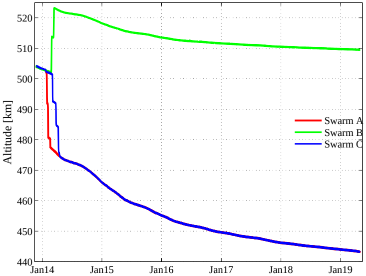

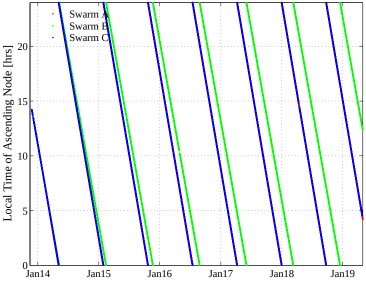

- Three identical satellites launched 22nd Nov 2013
- *Swarm* A, C now at altitude 440 km, longitudinal sep. ∼150 km
- *Swarm* B now at altitude 510 km
- Differential drift in local time, present separation 8 hrs

Time-dependent geomagnetic field modelling

- Potential field: $\mathbf{B} = -\nabla V$, internal part of the magnetic potential is parameterized as

$$V^{\text{int}} = a \sum_{n=1}^{N_{\text{int}}} \sum_{m=0}^{n} \left(g_n^m \cos m\phi + h_n^m \sin m\phi\right) \left(\frac{a}{r}\right)^{n+1} P_n^m \left(\cos\theta\right)$$

- For $n \leq 20$, expand in 6th order B-splines in time

$$g_n^m(t) = \sum_{k=1}^{K} {}^k g_n^m B_k(t).$$

Time-dependent geomagnetic field modelling

- Potential field: $\mathbf{B} = -\nabla V$, internal part of the magnetic potential is parameterized as

$$V^{\text{int}} = a \sum_{n=1}^{N_{\text{int}}} \sum_{m=0}^{n} \left(g_n^m \cos m\phi + h_n^m \sin m\phi\right) \left(\frac{a}{r}\right)^{n+1} P_n^m\left(\cos\theta\right)$$

- For $n \leq 20$, expand in 6th order B-splines in time

$$g_n^m(t) = \sum_{k=1}^{K} {}^{k}g_n^m B_k(t).$$

- Model parameters estimated by **regularized, robust, non-linear least squares** iteratively minimizing

$$\Theta = [\mathbf{d} - F(\mathbf{m})]^T \underline{\underline{\mathbf{W}}}[\mathbf{d} - F(\mathbf{m})] + \lambda_2 \mathbf{m}^T \underline{\underline{\mathbf{\Lambda}}}_2 \mathbf{m} + \lambda_3 \mathbf{m}^T \underline{\underline{\mathbf{\Lambda}}}_3 \mathbf{m}$$

Time-dependent geomagnetic field modelling

- Potential field: $\mathbf{B} = -\nabla V$, internal part of the magnetic potential is parameterized as

$$V^{\text{int}} = a \sum_{n=1}^{N_{\text{int}}} \sum_{m=0}^{n} \left(g_n^m \cos m\phi + h_n^m \sin m\phi \right) \left(\frac{a}{r} \right)^{n+1} P_n^m (\cos\theta)$$

- For $n \leq 20$, expand in 6th order B-splines in time

$$g_n^m(t) = \sum_{k=1}^{K} {}^k g_n^m B_k(t).$$

- Model parameters estimated by **regularized, robust, non-linear least squares** iteratively minimizing

$$\Theta = [\mathbf{d} - F(\mathbf{m})]^T \underline{\underline{\mathbf{W}}} [\mathbf{d} - F(\mathbf{m})] + \lambda_2 \mathbf{m}^T \underline{\underline{\mathbf{\Lambda}}}_2 \mathbf{m} + \lambda_3 \mathbf{m}^T \underline{\underline{\mathbf{\Lambda}}}_3 \mathbf{m}$$

- 11,652,019 data from geomagnetically quiet times, up to April 2019:
  Swarm: **MAG L1b 1Hz, version 0505** (vector & scalar field, along/across track diffs)
  + **CHAMP**, **Ørsted and SAC-C** satellite data
  + **Ground Observatory** Revised Monthly Means (based on AUX_OBS v. 0119 from BGS)

- *Swarm* non-polar, dark. scalar data misfit: **2.06 nT**, along-track diffs **0.25 nT**, cross-track diffs **0.41 nT**.
- `http://www.spacecenter.dk/files/magnetic-models/CHAOS-6/` [CHAOS-6-x9, *Finlay et al., 2016*]

Field intensity at Earth's surface

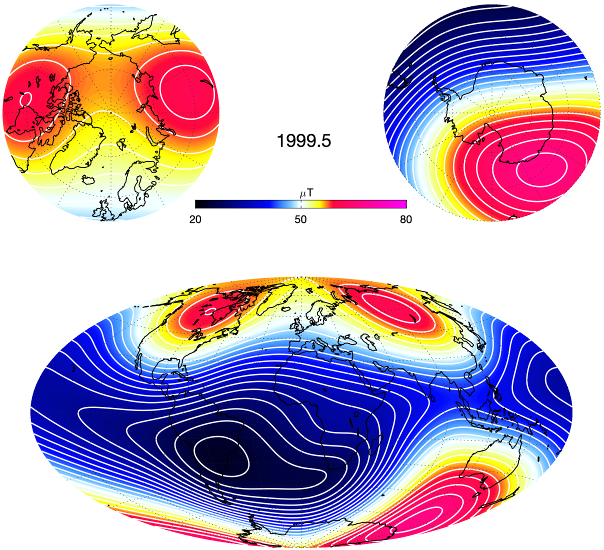

[Finlay et al., 2016 update, CHAOS-6-x9, to degree 20]

Field intensity at Earth's surface

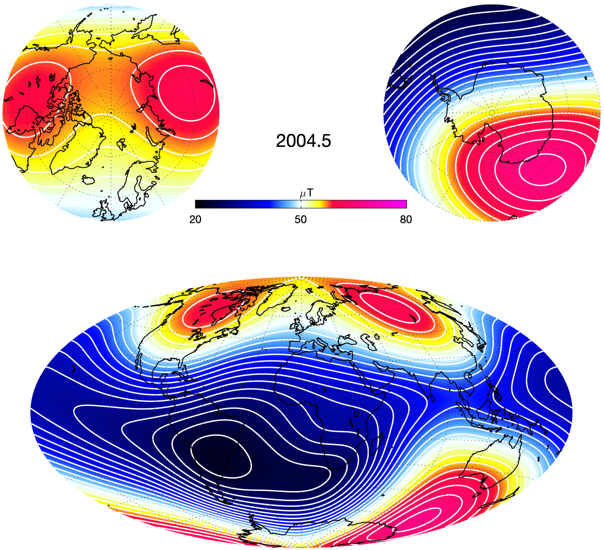

[Finlay et al., 2016 update, CHAOS-6-x9, to degree 20]

Field intensity at Earth's surface

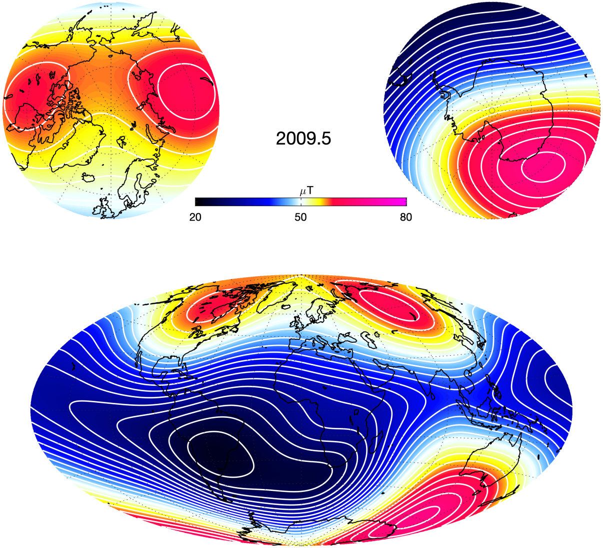

[Finlay et al., 2016 update, CHAOS-6-x9, to degree 20]

Field intensity at Earth's surface

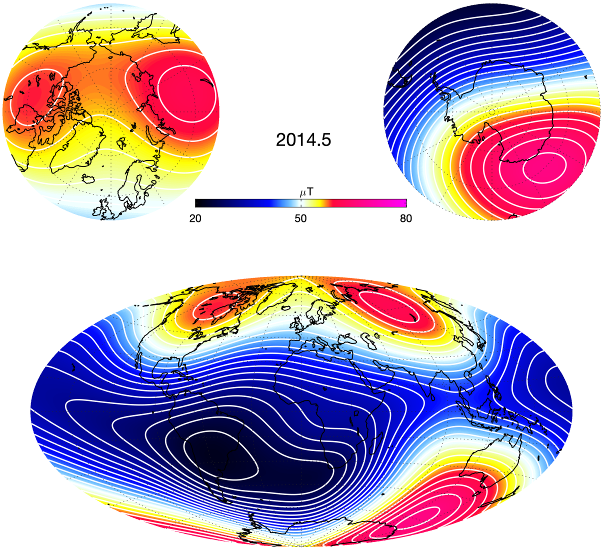

[Finlay et al., 2016 update, CHAOS-6-x9, to degree 20]

Field intensity at Earth's surface

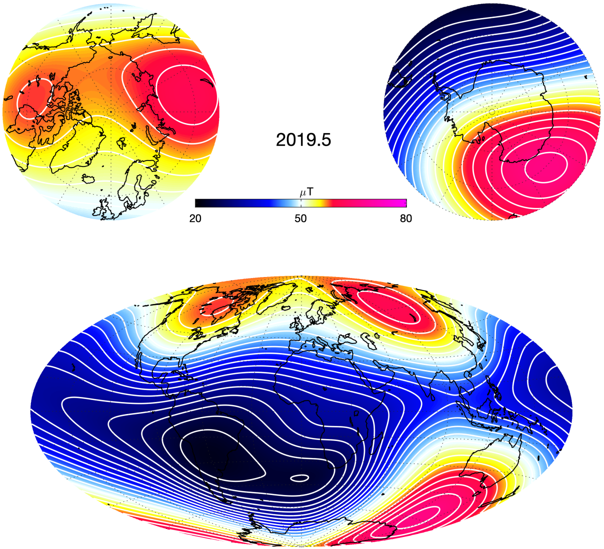

[Finlay et al., 2016 update, CHAOS-6-x9, to degree 20]

Linear motion of the North Magnetic Pole

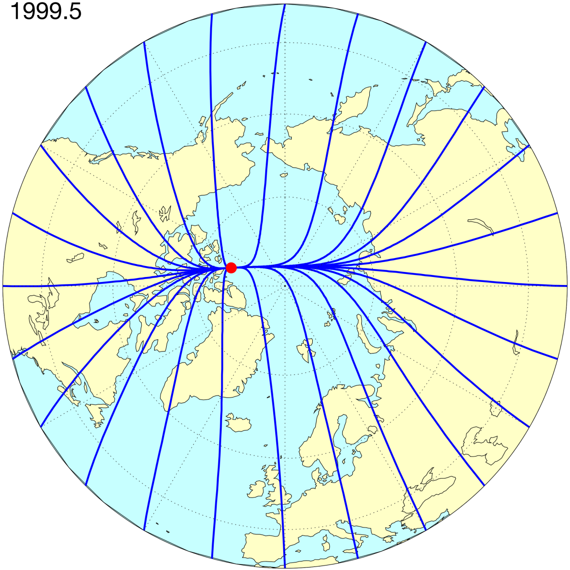

[Finlay et al., 2016 update, CHAOS-6-x9, to degree 20]

Linear motion of the North Magnetic Pole

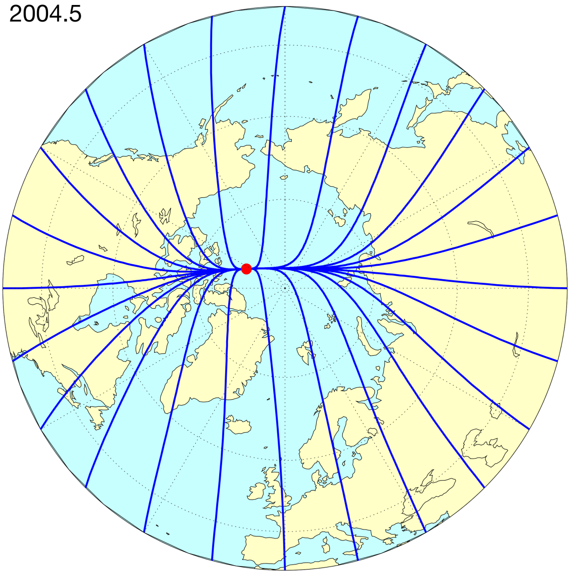

[Finlay et al., 2016 update, CHAOS-6-x9, to degree 20]

Linear motion of the North Magnetic Pole

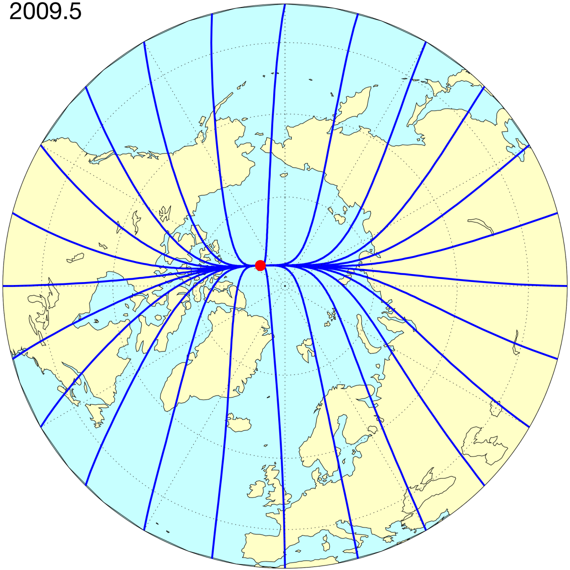

[Finlay et al., 2016 update, CHAOS-6-x9, to degree 20]

Linear motion of the North Magnetic Pole

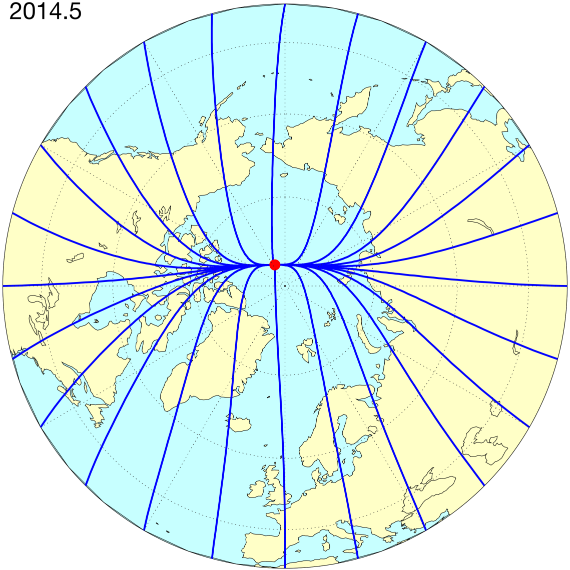

[Finlay et al., 2016 update, CHAOS-6-x9, to degree 20]

Linear motion of the North Magnetic Pole

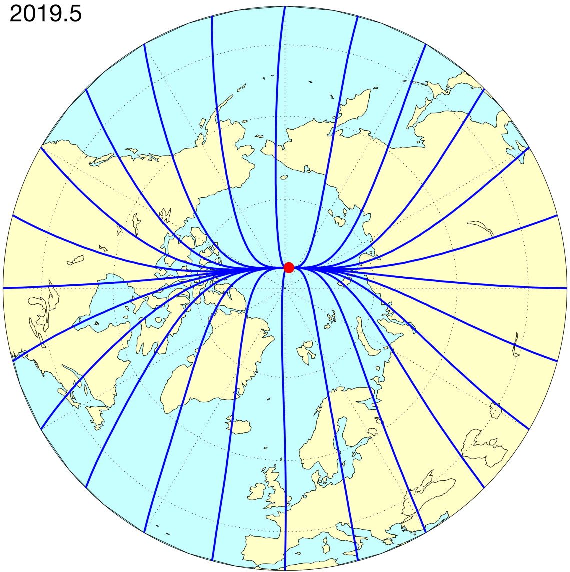

[Finlay et al., 2016 update, CHAOS-6-x9, to degree 20]

Due to changing balance between Canadian and Siberia flux patches

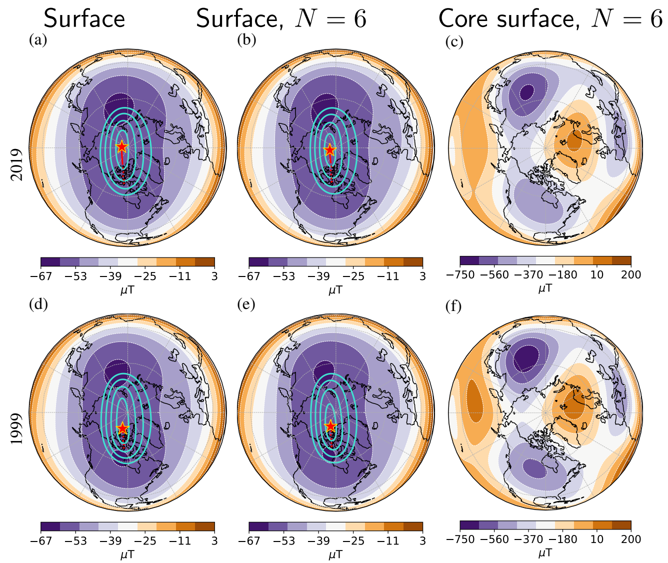

[Livermore and Finlay, under review]

Core origin: flux lobe elongation close to the tangent cylinder

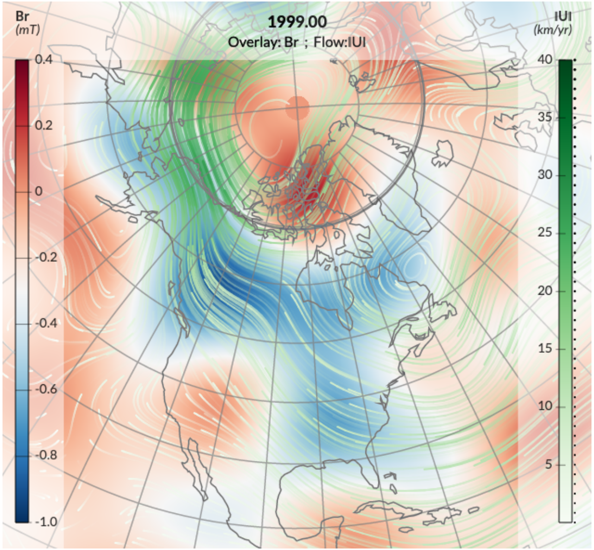

- Ensemble mean core surface flows
  [Barrois et al., 2017, 2018a, 2018b]
  Visualized using *webgeodyn* tool
  `https://geodyn.univ-grenoble-alpes.fr/`
  [Huder et al., 2019]
- Canadian flux lobe at core surface is being elongated
- Magnetic energy locally transfer from larger to smaller scales
- Causes the weakening of the N. American flux patch at surface
- Accounts for the majority of the NMP motion (961 km of the 1104 km moved 1999-2019.)

Core origin: flux lobe elongation close to the tangent cylinder

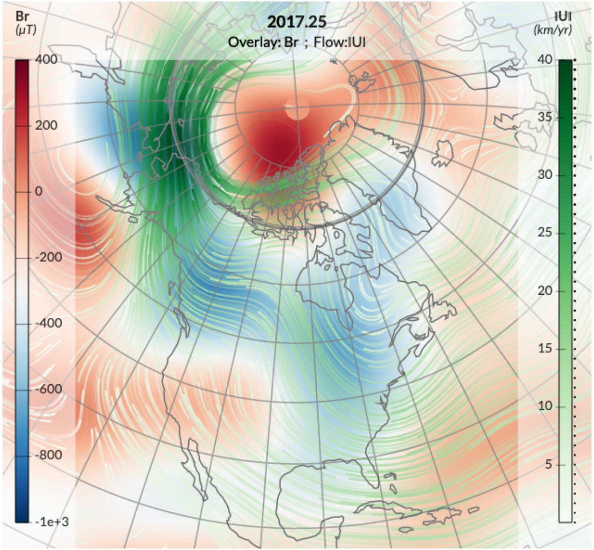

- Ensemble mean core surface flows
  [Barrois et al., 2017, 2018a, 2018b]
  Visualized using *webgeodyn* tool
  `https://geodyn.univ-grenoble-alpes.fr/`
  [Huder et al., 2019]
- Canadian flux lobe at core surface is being elongated
- Magnetic energy locally transfer from larger to smaller scales
- Causes the weakening of the N. American flux patch at surface
- Accounts for the majority of the NMP motion (961 km of the 1104 km moved 1999-2019.)

Spectra of Secular Variation and Acceleration power at core surface

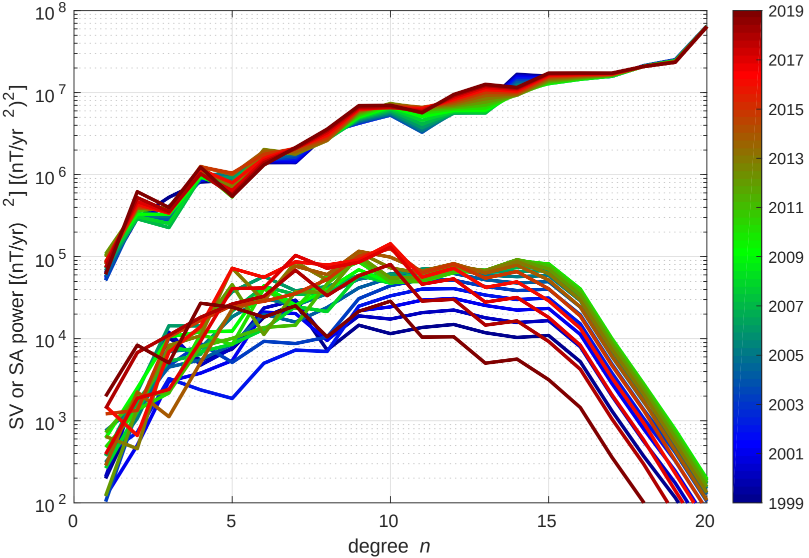

[Finlay et al., 2016 update, CHAOS-6-x9]

Core surface Secular Variation

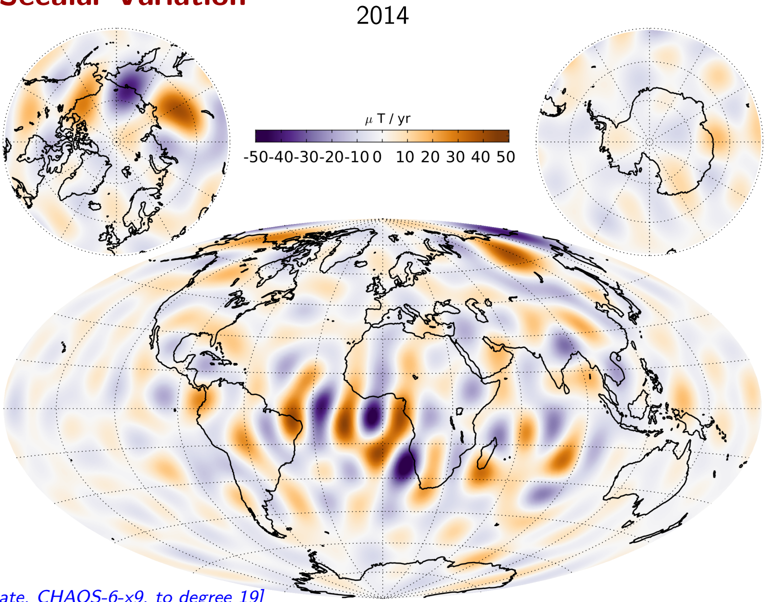

[Finlay et al., 2016 update, CHAOS-6-x9, to degree 19]

Core surface Secular Variation

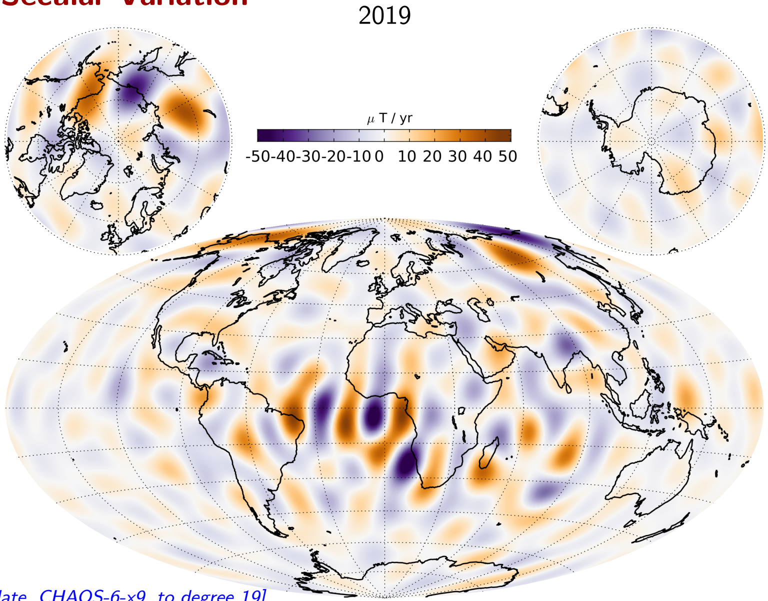

[Finlay et al., 2016 update, CHAOS-6-x9, to degree 19]

Core surface Secular Variation

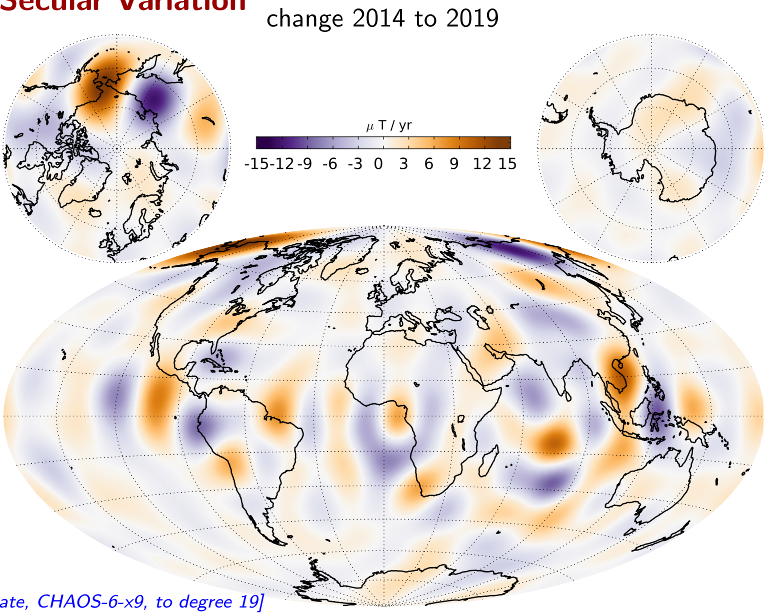

[Finlay et al., 2016 update, CHAOS-6-x9, to degree 19]

Core surface field accelerations in equatorial region

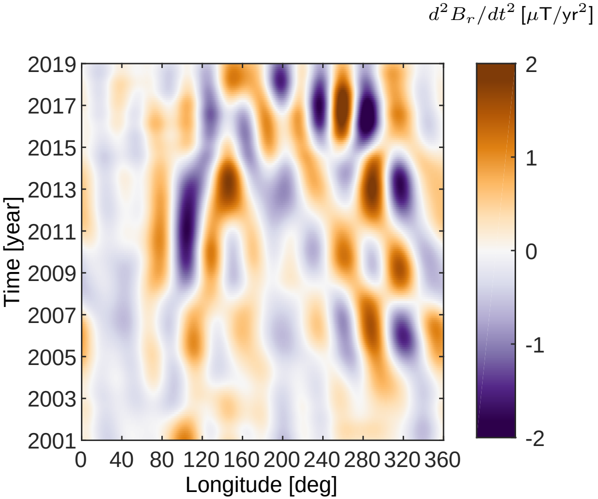

- Oscillations at some specific locations at core surface

[CHAOS-6-x9, to degree 10]

Core surface field accelerations in equatorial region

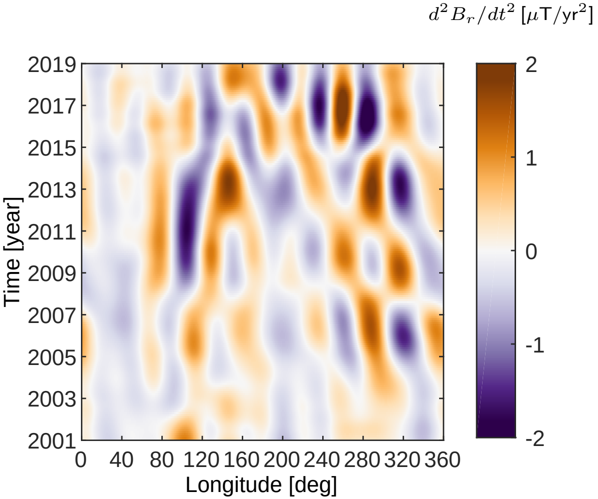

[CHAOS-6-x9, to degree 10]

- Oscillations at some specific locations at core surface
- Can be explained by non-axisymmetric azimuthal flow accelerations with alternating sign *[Kloss and Finlay, 2019]*

Core surface field accelerations in equatorial region

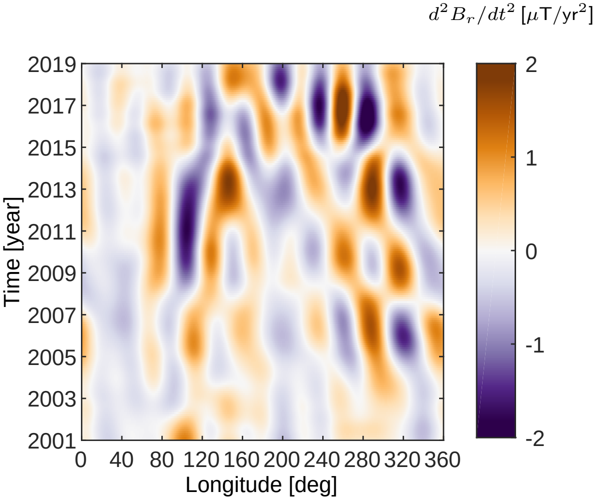

[CHAOS-6-x9, to degree 10]

- Oscillations at some specific locations at core surface
- Can be explained by non-axisymmetric azimuthal flow accelerations with alternating sign *[Kloss and Finlay, 2019]*
- Possibly also some fast propagating features?

Core surface field accelerations in equatorial region

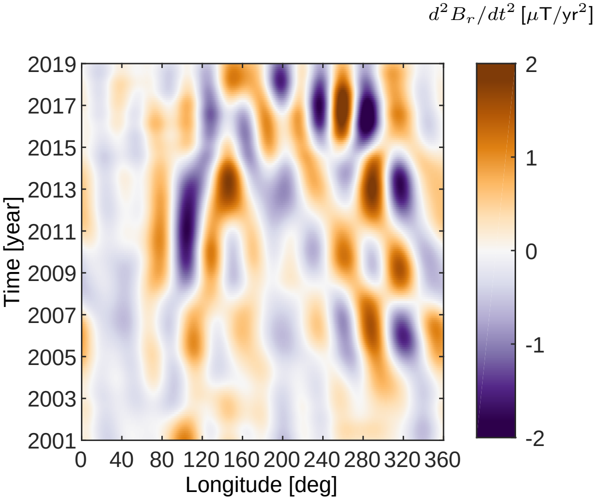

[CHAOS-6-x9, to degree 10]

- Oscillations at some specific locations at core surface
- Can be explained by non-axisymmetric azimuthal flow accelerations with alternating sign *[Kloss and Finlay, 2019]*

- Possibly also some fast propagating features?
- But this is a **spatially band-limited and temporally filtered** version of the truth *[Gillet, 2019]*

Core surface field accelerations in equatorial region

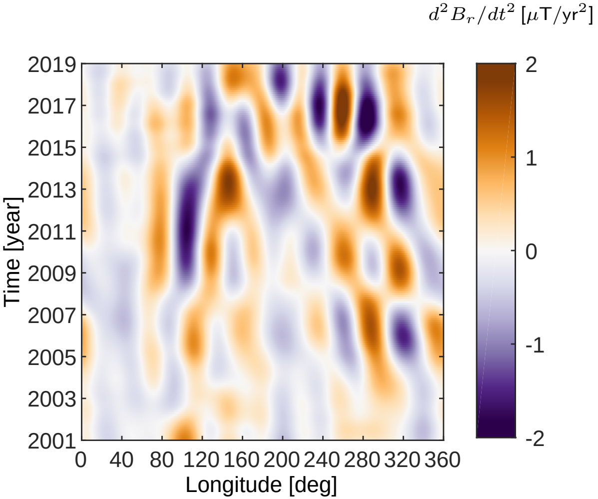

[CHAOS-6-x9, to degree 10]

- Oscillations at some specific locations at core surface
- Can be explained by non-axisymmetric azimuthal flow accelerations with alternating sign *[Kloss and Finlay, 2019]*

- Possibly also some fast propagating features?
- But this is a **spatially band-limited and temporally filtered** version of the truth *[Gillet, 2019]*
- Need to push to higher resolution in space and time to test whether features remain coherent....

Alternative local inversion method

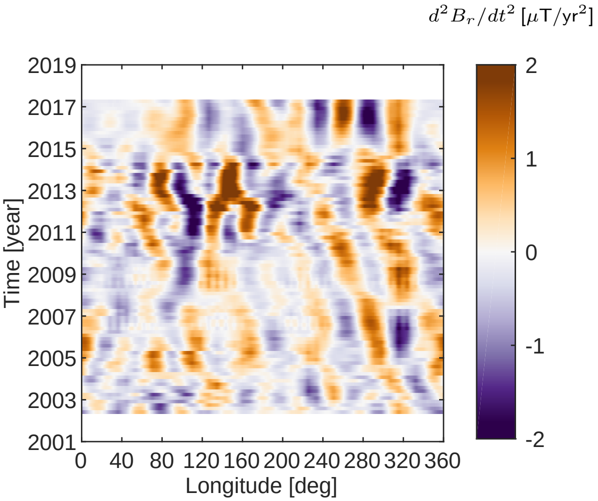

[SOLA, av. kernel width 42°, 2yr window, Hammer et al, in prep]

- Local inversion of *Swarm*, CHAMP, Cryosat data, with precisely known spatial & temporal av. functions *[Hammer and Finlay, 2019]*

Alternative local inversion method

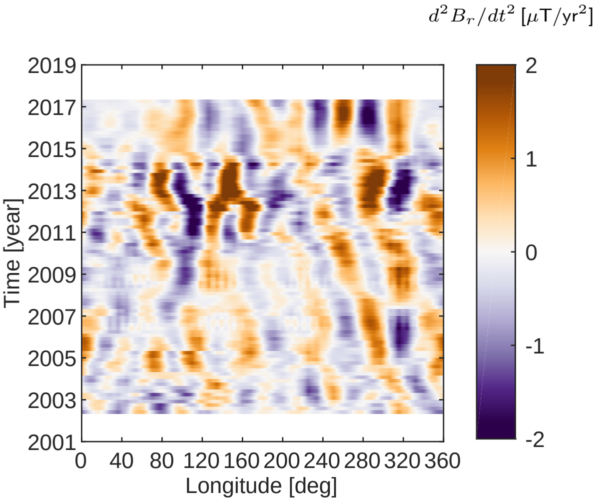

[SOLA, av. kernel width 42°, 2yr window, Hammer et al, in prep]

- Local inversion of *Swarm*, CHAMP, Cryosat data, with precisely known spatial & temporal av. functions *[Hammer and Finlay, 2019]*
- Use Green's fns, Laplaces's eqn with Neumann BC

$$d_i(\mathbf{r}_i) = \int_S G_i(\mathbf{r}_i, \mathbf{s}) B_r(\mathbf{s})\, dS$$

Alternative local inversion method

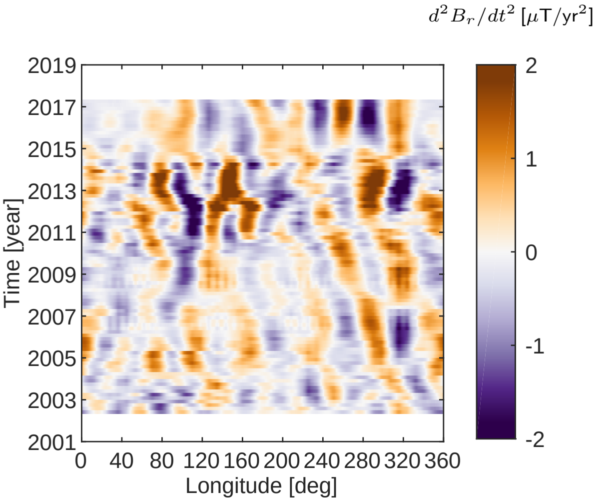

[SOLA, av. kernel width 42°, 2yr window, Hammer et al, in prep]

- Local inversion of *Swarm*, CHAMP, Cryosat data, with precisely known spatial & temporal av. functions *[Hammer and Finlay, 2019]*
- Use Green's fns, Laplaces's eqn with Neumann BC

$$d_i(\mathbf{r}_i) = \int_S G_i(\mathbf{r}_i, \mathbf{s}) B_r(\mathbf{s})\, dS$$

- Backus-Gilbert approach: write B_r at target location $\mathbf{s_0}$ on CMB as linear combination of data d_i

$$\widehat{B_r}(\mathbf{s_0}) = \sum_i q_i(\mathbf{s_0})\, d_i = \int_S \mathcal{K}(\mathbf{s_0}, \mathbf{s}) B_r(\mathbf{s}) dS$$

$$\text{where} \quad \mathcal{K}(\mathbf{s_0}, \mathbf{s}) = \sum_i q_i(\mathbf{s_0}) G_i(\mathbf{r_i}, \mathbf{s})$$

Alternative local inversion method

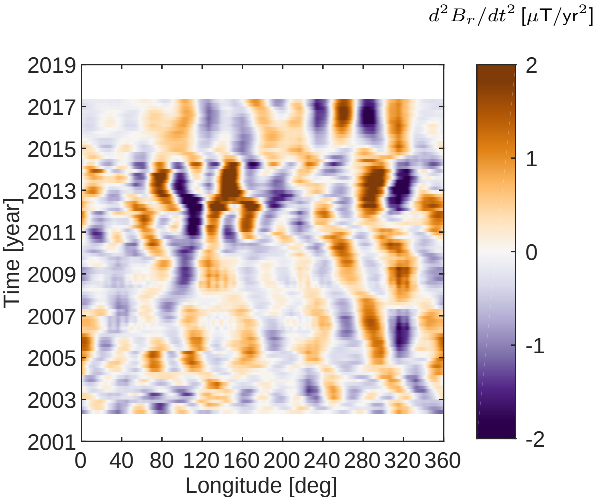

[SOLA, av. kernel width 42°, 2yr window, Hammer et al, in prep]

- Local inversion of *Swarm*, CHAMP, Cryosat data, with precisely known spatial & temporal av. functions *[Hammer and Finlay, 2019]*
- Use Green's fns, Laplaces's eqn with Neumann BC
$$d_i(\mathbf{r}_i) = \int_S G_i(\mathbf{r}_i, \mathbf{s}) B_r(\mathbf{s})\, dS$$
- Backus-Gilbert approach: write B_r at target location $\mathbf{s_0}$ on CMB as linear combination of data d_i
$$\widehat{B_r}(\mathbf{s_0}) = \sum_i q_i(\mathbf{s_0})\, d_i = \int_S \mathcal{K}(\mathbf{s_0}, \mathbf{s}) B_r(\mathbf{s}) dS$$
where $\quad \mathcal{K}(\mathbf{s_0}, \mathbf{s}) = \sum_i q_i(\mathbf{s_0}) G_i(\mathbf{r_i}, \mathbf{s})$
- Seek estimate with averaging Kernel as close as possible to idealized target $\mathcal{T}$ (SOLA)
$$\min \quad \oint_S [\mathcal{K}(\mathbf{s_0}, \mathbf{s}) - \mathcal{T}(\mathbf{s_0}, \mathbf{s})]^2 dS + \lambda \underline{\underline{E}}$$
subject to $\quad \int \mathcal{K}(\mathbf{s_0}, \mathbf{s})\, dS = 1$

A possible explanation: Arrival of QG Alfvén waves at core surface

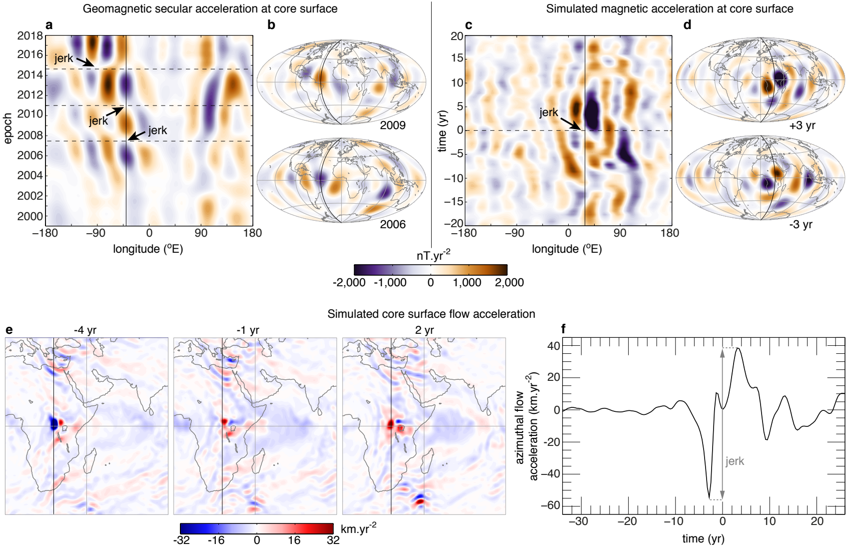

[Aubert and Finlay, 2019]

Summary

- Now $>$20 years of global magnetic field observations from space

Summary

- Now $>$20 years of global magnetic field observations from space

- Allowing us to track in detail changes in the core field:

  - Expansion of South Atlantic anomaly, North magnetic pole motion, weakening N. American flux patch
  - Sub-decadal, non-axisymmetric, fluctuations particularly at low latitudes

Summary

- Now >20 years of global magnetic field observations from space

- Allowing us to track in detail changes in the core field:
  - Expansion of South Atlantic anomaly, North magnetic pole motion, weakening N. American flux patch
  - Sub-decadal, non-axisymmetric, fluctuations particularly at low latitudes

- Improving constraints on core dynamics:
  - Decadal flow variability, especially close to inner core tangent cylinder
  - Possible indications of waves arriving at core surface, especially at low latitudes
  - New inversion schemes

Summary

- Now >20 years of global magnetic field observations from space
- Allowing us to track in detail changes in the core field:
  - Expansion of South Atlantic anomaly, North magnetic pole motion, weakening N. American flux patch
  - Sub-decadal, non-axisymmetric, fluctuations particularly at low latitudes
- Improving constraints on core dynamics:
  - Decadal flow variability, especially close to inner core tangent cylinder
  - Possible indications of waves arriving at core surface, especially at low latitudes
  - New inversion schemes
- Can look forward to further insights from
  - Lengthening time series provided by a long *Swarm* mission
  - Data from platform magnetometers improving knowledge of external current systems

  e.g. IRIDIUM, Spire Lemur nanosats, Cryosat, DMSP

Core surface field and flow

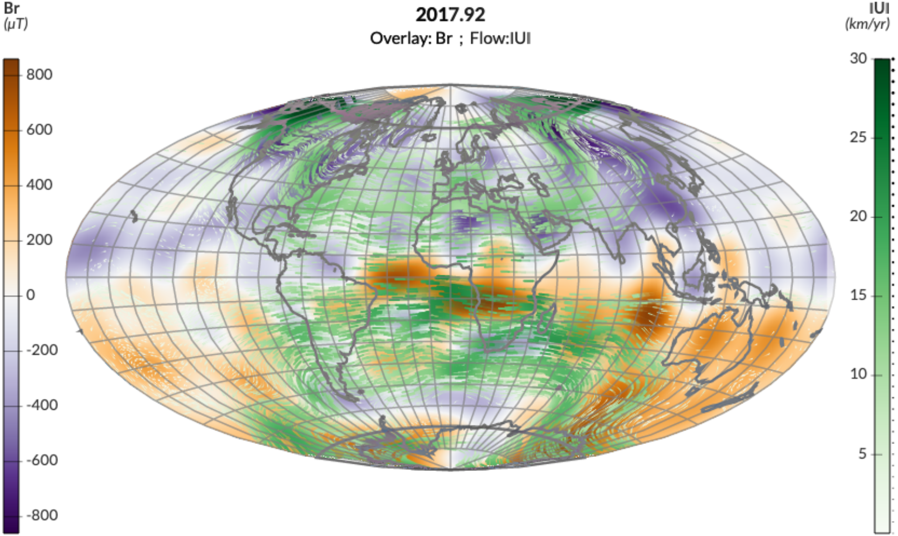

[Barrois et al, 2018b]

Azimuthal core flow accelerations of alternating sign

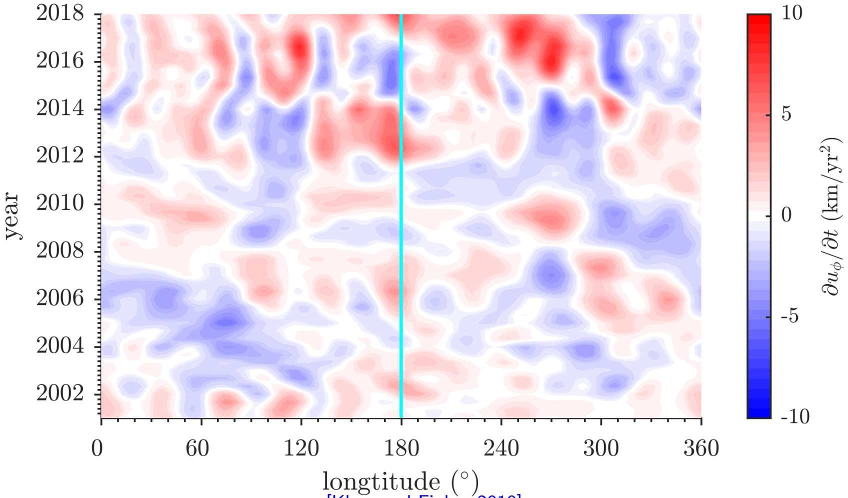

[Kloss and Finlay, 2019]

Core surface SA, Swarm-era, 1yr time windows

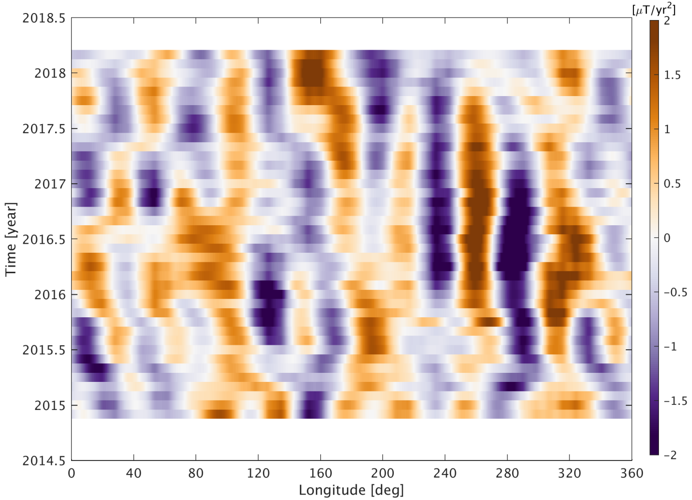

[Hammer et al, in prep]

CHAOS Field model: Parameterization

- **Potential field approach:** $\mathbf{B} = -\nabla V$ where $V = V^{\text{int}} + V^{\text{ext}}$.

- The internal part of the potential takes the form

$$V^{\text{int}} = a \sum_{n=1}^{N_{\text{int}}} \sum_{m=0}^{n} \left(g_n^m \cos m\phi + h_n^m \sin m\phi\right) \left(\frac{a}{r}\right)^{n+1} P_n^m(\cos\theta)$$

- For $n \leq 20$, expand in 6th order B-splines

$$g_n^m(t) = \sum_{k=1}^{K} {}^k g_n^m B_k(t).$$

- Expand external potential in SM and GSM coordinates, with θ_d and T_d being dipole co-lat. and local time

$$\begin{aligned} V^{\text{ext}} &= a \sum_{n=1}^{2} \sum_{m=0}^{n} \left(q_n^m \cos mT_d + s_n^m \sin mT_d\right) \left(\frac{r}{a}\right)^{n} P_n^m(\cos\theta_d) \\ &+ a \sum_{n=1}^{2} q_n^{0,\text{GSM}} R_n^0(r,\theta,\phi). \end{aligned}$$

[Olsen et al, 2006, 2014]

Subtractive Optimized Local Analysis (SOLA)

- Forward scheme:

$$d_n(\mathbf{r_n}) = \int_S G_n(\mathbf{r_n}, \mathbf{s}) B_r(\mathbf{s}) dS$$

where G_n is the Green's function for the Neumann boundary value problem relating $B_r(\mathbf{s})$ on S to data d_n.

- Estimate the field at a location of interest $\mathbf{s_0}$ on S using

$$\widehat{B_r}(\mathbf{s_0}) = \sum_n q_n(\mathbf{s_0}) d_n = \sum_n q_n(\mathbf{s_0}) \int_S G_n(\mathbf{r_n}, \mathbf{s}) B_r(\mathbf{s}) dS = \int_S \mathcal{K}(\mathbf{s_0}, \mathbf{s} | \mathbf{r_n}) B_r(\mathbf{s}) dS$$

where $\mathcal{K}$ is a 'Resolution Kernel', describing how the estimate is a averaged version of the true $B_r(\mathbf{s_0})$

$$\mathcal{K}(\mathbf{s_0}, \mathbf{s}) = \sum_n q_n(\mathbf{s_0}) G_n(\mathbf{r_n}, \mathbf{s})$$

- SOLA: Subtractive Optimized Local Average: find q_n such that $\mathcal{K}$ is as close as possible to a target Kernel $\mathcal{T}$

$$\min \quad \oint_S [\mathcal{K}(\mathbf{s_0}, \mathbf{s}) - \mathcal{T}(\mathbf{s_0}, \mathbf{s})]^2 dS + \lambda \underline{\underline{E}} \quad \text{subject to} \quad \int \mathcal{K}(\mathbf{s_0}, \mathbf{s})\, dS = 1$$

- Variance on the estimate is obtained as

$$\sigma^2(\mathbf{s_0}) = \mathbf{q}^T \underline{\underline{E}} \mathbf{q}$$